Establishing a Customized Guide Plate for Osteotomy in Total Knee Arthroplasty Using Lower-extremity X-ray and Knee Computed Tomography Images

Jin Zhang[1], Xiao-Bin Tian[2], Li Sun[2], Ru-Yin Hu[2], Jia-Liang Tian[2], Wei Han[2], Jin-Min Zhao[1]

[1]Department of Orthopedics, The First Affiliated Hospital of Guangxi Medical University, Nanning, Guangxi 530021, China
[2]Department of Orthopedics, Guizhou Provincial People's Hospital, Guiyang, Guizhou 550002, China

Jin Zhang and Xiao-Bin Tian contributed equally to this work.

Abstract

Background: The conventional method cannot guarantee the precise osteotomies required for a perfect realignment and a better prognosis after total knee arthroplasty (TKA). This study investigated a customized guide plate for osteotomy placement in TKAs with the aid of the statistical shape model technique using weight-bearing lower-extremity X-rays and computed tomography (CT) images of the knee.
Methods: From October 2014 to June 2015, 42 patients who underwent a TKA in Guizhou Provincial People's Hospital were divided into a guide plate group (GPG, 21 cases) and a traditional surgery group (TSG, 21 cases) using a random number table method. In the GPG group, a guide plate was designed and printed using preoperative three-dimensional measurements to plan and digitally simulate the operation. TSG cases were treated with the conventional method. Outcomes were obtained from the postoperative image examination and short-term follow-up.
Results: Operative time was 49.0 ± 10.5 min for GPG, and 62.0 ± 9.7 min in TSG. The coronal femoral angle, coronal tibial angle, posterior tibial slope, and the angle between the posterior condylar osteotomy surface and the surgical transepicondylar axis were 89.2 ± 1.7°, 89.0 ± 1.1°, 6.6 ± 1.4°, and 0.9 ± 0.3° in GPG, and 86.7 ± 2.9°, 87.6 ± 2.1°, 8.9 ± 2.8°, and 1.7 ± 0.8° in TSG, respectively. The Hospital for Special Surgery scores 3 months after surgery were 83.7 ± 18.4 in GPG and 71.5 ± 15.2 in TSG. Statistically significant differences were found between GPG and TSG in all measurements.
Conclusions: A customized guide plate to create an accurate osteotomy in TKAs may be created using lower-extremity X-ray and knee CT images. This allows for shorter operative times and better postoperative alignment than the traditional surgery. Application of the digital guide plate may also result in better short-term outcomes.

Key words: Digital; Guide Plate for Osteotomy; Lower-extremity X-ray; Statistical Shape Model; Total Knee Arthroplasty

Introduction

Total knee arthroplasty (TKA) is an effective treatment for knee joint diseases such as osteoarthritis and rheumatoid arthritis. The perfect reconstruction of lower limb alignment plays a very important role in the outcomes of knee joint replacement, and can affect both symptom relief and the life time of the prosthesis.[1,2]

The traditional method for a correctional osteotomy is to use the lower-extremity weight-bearing full-length X-ray to determine the osteotomy location and the angle of the coronal plane. As the accuracy of measuring the joint center with two-dimensional (2D) images cannot be guaranteed, the preoperative osteotomy position and angle planning with these images are imprecise. The angle of the sagittal and transverse plane depends on the surgeon's experience. A prolonged operative time and poor accuracy are inevitable.[3]

With the development of digital technology, the clinical applications of three-dimensional (3D) measurement and

Access this article online	
Quick Response Code:	Website: www.cmj.org
	DOI: 10.4103/0366-6999.176082

Address for correspondence: Dr. Jin-Min Zhao, Department of Orthopedics, The First Affiliated Hospital of Guangxi Medical University, Nanning, Guangxi 530021, China
E-Mail: zhaojinmin@126.com

Received: 02-11-2015 **Edited by:** Li-Shao Guo
How to cite this article: Zhang J, Tian XB, Sun L, Hu RY, Tian JL, Han W, Zhao JM. Establishing a Customized Guide Plate for Osteotomy in Total Knee Arthroplasty Using Lower-extremity X-ray and Knee Computed Tomography Images. Chin Med J 2016;129:386-91.

operative simulation have gradually increased. In our study, calibrated lower-extremity weight-bearing full-length X-rays and computed tomography (CT) scans of the knee were collected. The statistical shape model (SSM) technique was used to synthesize a 3D model of the knee from the X-ray. A 3D model of the lower limb can be generated with the use of the 3D knee model created using the SSM technique along with CT scans. After the hip and ankle centers were determined on the dual plane X-ray, the relative positional relationship between the two joint centers and the 3D knee model was measured. Using this method, a preoperative analysis can be conducted on the basis of weight-bearing function, avoiding the significant radiation exposure due to CT scan. The preoperative planning, osteotomy simulation, and prosthetic placement were performed. The 3D-printed osteotomy guide plate from the digitally designed model was applied to the TKA.

Methods

This clinical trial received permission from the Ethics Committee of Guizhou Provincial People's Hospital, and all patients and their families signed informed consents. A total of 42 cases of osteoarthritis in patients who previously underwent a unilateral TKA at Guizhou Provincial People's Hospital from October 2014 to June 2015 were enrolled in our study. Of these patients, 17 were male, and 25 were female. The involved knee was on the left in 20 cases, while 22 were on the right. Average age was 62 ± 7 years. Preoperative mean body mass index was 25.3 ± 6.4 kg/m^2. The eligibility criteria included: (1) unilateral TKA; (2) varus deformity of the operative knee; (3) osteoarthritis of the operative knee. Exclusion criteria included: (1) severe comorbidities that may prolong hospitalization time; (2) severe osteoporosis; (3) the patient declined to participate in the research. Patients were divided into two groups: A guide plate group (GPG, 21 cases), and a traditional surgery group (TSG, 21 cases), using the random number table method. In GPG patients, preoperative thin slice CT scans of the knee were obtained using the Siemens 64 row spiral CT (Siemens, Munich, Germany). The scanning voltage was 130 kV, the scanning thickness was 1 mm, and the matrix was 512 × 512. Digital Imaging and Communications in Medicine format CT data were imported into Simpleware 7.2 (Simpleware Ltd., Exeter, UK) to reconstruct the 3D stereolithography format knee model. Calibrated weight-bearing full-length dual plane knee X-ray images were obtained [Figures 1 and 2]. 3D knee models were synthesized from calibrated dual plane images with SSM of the knee and registration.[4-7] The automatic registration of the 3D knee model from the CT scan and from the SSM technique can be obtained digitally [Figure 3].

The hip center (center of the synthesized sphere) and the ankle center (center of the talar articular surface) were determined. Through the position relationship between the centers, points on the calibration device and the X-ray source, the relative spatial relationship between the two central points and the 3D model of the knee joint was determined. The central point of the distal femur was defined as the midpoint of the Whiteside line.[8] The central point of the proximal tibia was defined as the center of the tibial intercondylar eminence. The femoral anatomic axis was defined as the connection between the central point of the distal femur and the medullary cavity center 10 cm above the knee joint space. The femoral mechanical axis was defined as the connection between the central point of the distal femur and the central point of the femoral head. The mechanical axis of the tibia was defined as the connection between the central point of the proximal tibia and the central point of the ankle joint.

Prosthetic models were obtained by 3D scanning the NexGen LPS (Zimmer Biomet, Warsaw, Indiana, USA) with the Laser-RE (Serein Precision Machinery Company, Shenzhen, China).

The femoral distal osteotomy valgus angle was the angle measured between the femoral anatomy and the mechanical axis, while the osteotomy thickness was 9 mm from the lowest point of the medial femoral condyle.

Through the simulated operation, we were able to choose the suitable size of the prosthesis. The osteotomy line of the anterior and posterior condyles was parallel to the surgical transepicondylar axis (STEA) [Figure 4].

The proximal tibial osteotomy line was perpendicular to the mechanical axis on the coronal plane, and was 7° posterior slope on the sagittal plane resulting from the design of the prosthesis. The thickness of the proximal tibial osteotomy was 10 mm from the highest point of the lateral tibial condyle.

According to the design above and the operative simulation, the hole position of the nonheaded screw and the size of the prosthesis were determined. The base of the guide plate was reverse engineered in accordance with the shape of the distal femur and proximal tibia. The screw hole and the base were then connected. The digital design was created using Geomagic (3D Systems, Valencia, CA, USA). In the reverse design stage of the base, the more shape characteristic

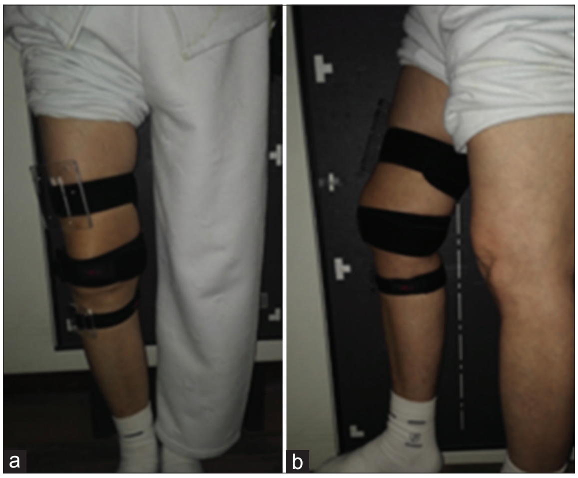

Figure 1: Photo of calibrated leg. (a) Frontal view. (b) Lateral view.

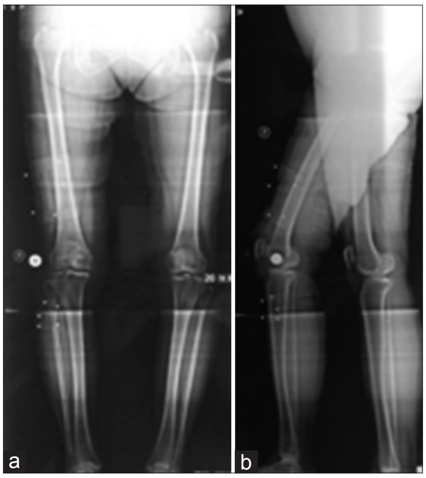

Figure 2: X-ray images of calibrated weight-bearing full-length lower limb. (a) Anteroposterior image. (b) Lateral image.

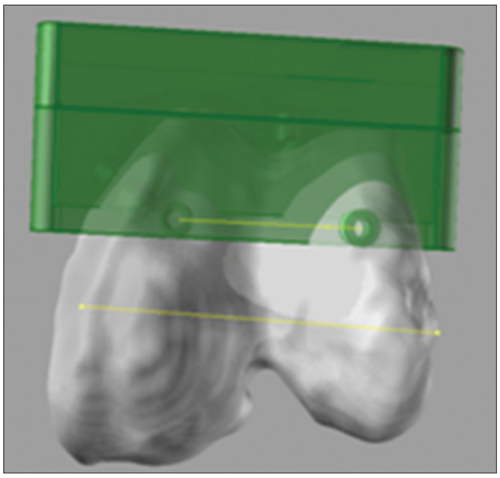

Figurer 4: Anterior and posterior condylar osteotomy line is parallel to surgical transepicondylar axis.

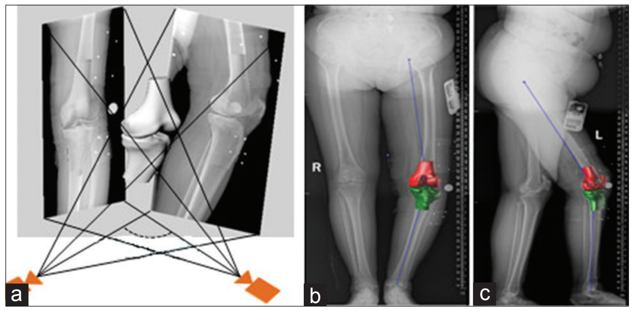

Figure 3: Registration between the three-dimensional model synthesized from calibrated X-ray and three-dimensional model from computed tomography. (a) The three dimensional diagrammatic sketch of registration. (b) The anteroposterior film after registration. (c) The lateral film after registration.

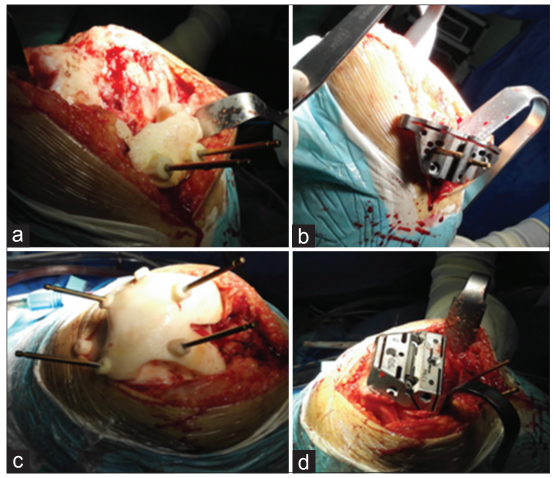

Figure 5: The nonhead screws' positions were determined according the guide plates in order to locate the osteotomy devices. (a) The guide plate determined the positions of the nonhead screws in the proximal tibia. (b) The nonhead screws determined the positions of the proximal tibial osteotomy divices. (c) The guide plate determined the positions of the nonhead screws in the distal femur. (d)The nonhead screws determined the positions of the anterior and posterior condylar osteotomy divices.

bone surface was selected to be the attachment area for the guide plate to obtain a better match for the installation. The guide plate was 3D-printed with the polylactic acid material using a 3D Printer (3D Systems Company, Rock Hill, South Carolina, USA). After the operative exposure, the guide plates were attached to the bony surface where the articular cartilage was removed to determine the position of the nonheaded screw for the distal femoral, anterior and posterior condylar, and proximal tibial osteotomy devices. All surgeries were performed by a single surgeon [Figure 5]. Postoperative radiographs were obtained to verify the alignment of the reconstruction [Figure 6].

In the TSG, the angle between the femoral anatomic and mechanical axis was measured preoperatively using a weight-bearing full-length lower-extremity X-ray. The valgus angle for the distal femoral osteotomy was chosen using the closest available angle on the surgical instruments. The intramedullary alignment guide was applied to the femur while the extramedullary alignment guide was applied to the tibia. The rotational angle was chosen according to the experience of the surgeon.

Obtained data were statistically analyzed using SPSS 16.0 (IBM, Armonk, NY, USA). A *t*-test was applied to assess for differences between groups, with $P < 0.05$ considered significant.

Results

The operation time was 49.0 ± 10.5 min for GPG, and 62.0 ± 9.7 min for TSG. The coronal femoral angle, coronal tibial angle, posterior tibial slope, and the angle between the posterior condylar osteotomy surface and the STEA were 89.2 ± 1.7°, 89.0 ± 1.1°, 6.6 ± 1.4°, and 0.9 ± 0.3° in GPG, and 86.7 ± 2.9°, 87.6 ± 2.1°, 8.9 ± 2.8°, and 1.7 ± 0.8° in TSG, respectively. The Hospital for Special Surgery knee scores 3 months after surgery were 83.7 ± 18.4 after GPG and 71.5 ± 15.2 after TSG, respectively. Statistically significant differences were found between all previously noted comparisons [Table 1].

Table 1: Comparing the outcomes of the GPG and the TSG

Items	GPG	TSG	*t*	*P*
Operation time (min)	49.0 ± 10.5	62.0 ± 9.7	−16.53	0.018
Coronal femoral angle (°)	89.2 ± 1.7	86.7 ± 2.9	2.57	0.036
Coronal tibial angle (°)	89.0 ± 1.1	87.6 ± 2.1	2.42	0.023
Posterior tibial slope (°)	6.6 ± 1.4	8.9 ± 2.8	−19.35	0.013
Angle between posterior condylar osteotomy surface and the STEA (°)	0.9 ± 0.3	1.7 ± 0.8	−26.37	0.009
HSS score 3 months after surgery	83.7 ± 18.4	71.5 ± 15.2	3.31	0.029

HSS: Hospital for Special Surgery; GPG: Guide plate group; TSG: Traditional surgery group; STEA: Surgical transepicondylar axis.

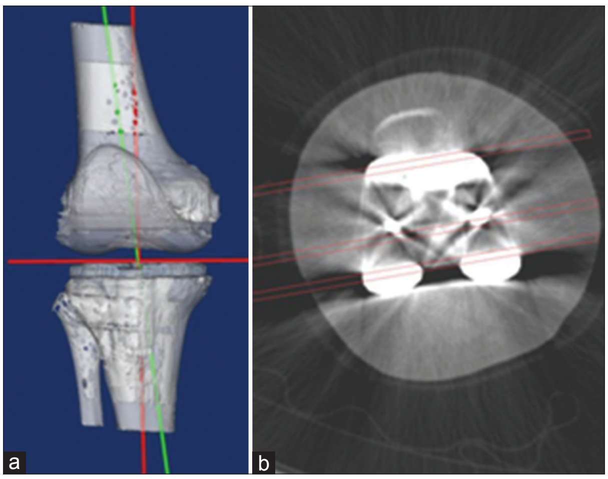

Figure 6: Postoperative coronal femoral/tibial angles and the angle between posterior condylar osteotomy surface and the surgical transepicondylar axis. (a) The postoperative coronal femoral/tibial angles were 90°. (b) The postoperative angle between posterior condylar osteotomy surface and the surgical transepicondylar axis was 0°.

Discussion

TKA is an effective treatment for severe knee diseases. An accurate osteotomy and the reconstruction of the normal alignment of the lower limbs are key to obtaining a good curative effect.[1,2] There is significant anatomic variation of the knee joint, especially in the southwest part of China. The knee joint prosthesis and the matching operative instruments are designed with the anatomic characteristics of the European and American knee joint in mind. There may therefore be a large error when using conventional osteotomy instruments in East Asia, resulting in poor alignment of the lower limb, early component loosening, pain, activity limitation, and other complications. The traditional surgical osteotomy is based on the measurement of the weight-bearing full-length lower-extremity X-ray and the intra/extramedullary alignment guides. There is significant subjectivity when using these measurements. This increases the potential risk of infection, bleeding, and fat embolism in the traditional intramedullary alignment guide-based surgery.[9,10]

Modern computer technology has developed rapidly, providing a platform for preoperative planning. The orthopedic surgeon can perform computer-assisted precise operative measurements.[11-13] Hafez *et al*.[14] digitally designed and 3D printed the osteotomy guide plate for a TKA for the first time, which can effectively avoid the fat embolisms that often result from the placement of the intramedullary alignment guide. Cai *et al*.[15] uses digital technology to control the axial alignment of total knee arthroplasties, but they needed a CT of the full-length lower limb. Zhang *et al*.[16] synthesized a 3D joint model from hip, knee, and ankle CTs and a weight-bearing full-length X-ray. 3D alignment reconstruction and the determination of the femoral prosthetic valgus angle can be made using the preoperative design based on the 3D model of the lower limb. In this study, the measurement and reconstruction of the alignment was conducted under physiologic load to be more consistent with normal biomechanical characteristics. However, it required a thin-cut CT scan of the three joints, which significantly increased the examination cost and the patient's radiation exposure.

In this study, the use of advanced 3D synthesis and 2D/3D registration technology allowed for the reconstruction of a weight-bearing 3D model of the lower limb, which was used to achieve an accurate 3D measurement of the coronal, sagittal and transversal plane, and to minimize medical expense and X-ray exposure. Our outcomes suggest that the customized guide plate can increase the accuracy of the operation, shorten operative times, and decrease the complications that can result from intramedullary alignment guide placement.

In digital medical studies, the 2D/3D registration of image data is accurate and important.[17-20] With the increased use of low-dose radiation imaging equipment in recent years, 2D/3D registration of X-ray and CT highlights the advantages.[21,22] The construction of a 3D bone shape model plays an important role in both surgical navigation and image-based studies of the kinematics of the knee joint *in vivo*.[23-25] In our study, the calibrated dual plane X-ray images were used to synthesize the SSM to conduct the feature-based registration of a 3D model from the CT. Although 2D/3D registration could be obtained by using a single plane X-ray, the accuracy of a single plane X-ray is far inferior to that of a dual plane X-ray.[26,27] Li *et al*.[27] used a dual fluoroscopic imaging system in a kinematic study of the knee joint *in vivo*. Van de Velde *et al*.[28] also took the attitude that the 3D model could be registered with a single plane X-ray, but overall accuracy of this approach is much lower than that obtained with the dual plane X-ray. Zhu and Li[29] held the view that in the 2D/3D registration, the accuracy gap in the synthesized distal femur model between single plane and dual plane X-rays is significant, while there is almost no gap between dual plane X-rays and mutual plane X-rays. A number of studies have demonstrated that the irregularities in the 3D model created using a dual plane X-ray can be accepted in the medical field. Zhu *et al*.[29] introduced a technique to predict the 3D model of the distal femur. The deviation between the predicted 3D model and the model reconstructed from 3D medical images was <0.2 mm. Wang *et al*.[30] also applied the dual fluoroscopic image matching method in their study of *in vivo* spinal kinematics. The average positional deviation was 0.2 mm, and the average angular deviation was 0.4°. The repeatability was high. Baka *et al*.[31] indicated that the deviation between the distal femur model synthesized from dual plane X-rays and the 3D model reconstructed from the CT was <1.68 mm. Zheng *et al*.[32] confirmed the feasibility of this 2D/3D registration method. They also created the surface shape model from calibrated X-rays to conduct feature-based registration.

This study is a preliminary evaluation of a digitally customized osteotomy guide plate for TKA. The limitation of an insufficient sample size in this study may result in unnecessary variation. Future work will also add a cartilage model to the bony knee 3D model to decrease variability and reduce the surgical task of removing the articular cartilage. However, our findings suggest that the indications for a guide plate should be expanded, especially in cases of severe intra-or extra-articular deformity, given its customized and minimally invasive nature.

Financial support and sponsorship

This work was supported by grants from Special Fund for Culture of Top Young Scientific Talents in Guizhou Province (No. 2011-30), Projects of Science and Technology of Guizhou Province (No. SY[2015] 3044), Fund of Youth of Guizhou Provincial People's Hospital (No. GZSYQN[2015] 05) and Medical Scientific Research Foundation of Guizhou Province (No. gzwjkj2015-1-018).

Conflicts of interest

There are no conflicts of interest.

References

1. Kirill G, Mounim K, Morten GT, Henrik H, Anders T. What is the optimal alignment of the tibial and femoral components in knee arthroplasty? Acta Orthop Belg 2014;85:480-7. doi: 10.3109/17453674.2014.940573.
2. Michael B. Consequences of malalignment in total knee arthroplasty: Few if any-opposes. Semin Arthroplasty 2010;21:99-101. doi: 10.1053/j.sart.2009.12.009.
3. Ferrara F, Cipriani A, Magarelli N, Rapisarda S, De Santis V, Burrofato A, *et al.* Implant positioning in TKA: Comparison between conventional and patient-specific instrumentation. Orthopedics 2015;38:e271-80. doi: 10.3928/01477447-20150402-54.
4. Li JS, Tsai TY, Wang S, Li P, Kwon YM, Freiberg A, *et al.* Prediction of *in vivo* knee joint kinematics using a combined dual fluoroscopy imaging and statistical shape modeling technique. J Biomech Eng 2014;136:124503. doi: 10.1115/1.4028819.
5. Tsai TY, Li JS, Wang S, Li P, Kwon YM, Li G. Principal component analysis in construction of 3D human knee joint models using a statistical shape model method. Comput Methods Biomech Biomed Engin 2015;18:721-9. doi: 10.1080/10255842.2013.843676.
6. Li G, Wang S, Passias P, Xia Q, Li G, Wood K. Segmental *in vivo* vertebral motion during functional human lumbar spine activities. Eur Spine J 2009;18:1013-21. doi: 10.1007/s00586-009-0936-6.
7. Wang S, Xia Q, Passias P, Wood K, Li G. Measurement of geometric deformation of lumbar intervertebral discs under *in-vivo* weightbearing condition. J Biomech 2009;42:705-11. doi: 10.1016/j.jbiomech.2009.01.004.
8. Whiteside LA, Arima J. The anteroposterior axis for femoral rotational alignment in valgus total knee arthroplasty. Clin Orthop Relat Res 1995;321:168-72.
9. Lee SC, Yoon JY, Nam CH, Kim TK, Jung KA, Lee DW. Cerebral fat embolism syndrome after simultaneous bilateral total knee arthroplasty: A case series. J Arthroplasty 2012;27:409-14. doi: 10.1016/j.arth.2011.06.013.
10. Zhao J, Zhang J, Ji X, Li X, Qian Q, Xu Q. Does intramedullary canal irrigation reduce fat emboli? A randomized clinical trial with transesophageal echocardiography. J Arthroplasty 2015;30:451-5. doi: 10.1016/j.arth.2014.10.006.
11. Takeyasu Y, Oka K, Miyake J, Kataoka T, Moritomo H, Murase T. Preoperative, computer simulation-based, three-dimensional corrective osteotomy for cubitus varus deformity with use of a custom-designed surgical device. J Bone Joint Surg Am 2013;95:1731-9. doi: 10.2106/JBJS.L.01622.
12. Dérand P, Rännar LE, Hirsch JM. Imaging, virtual planning, design, and production of patient-specific implants and clinical validation in craniomaxillofacial surgery. Craniomaxillofac Trauma Reconstr 2012;5:137-44. doi: 10.1055/s-0032-1313357.
13. Chen YX, Zhang K, Hao YN, Hu YC. Research status and application prospects of digital technology in orthopaedics. Orthop Surg 2012;4:131-8. doi: 10.1111/j.1757-7861.2012.00184.x.
14. Hafez MA, Chelule KL, Seedhom BB, Sherman KP. Computer-assisted total knee arthroplasty using patient-specific templating. Clin Orthop Relat Res 2006;444:184-92. doi: 10.1097/01.blo.0000201148.06454.ef.
15. Cai JF, Yuan F, Ma M, Luo SL, Zhou W, Wu Q, *et al*. Application of digital technology in control of femoral axial alignment in personalized total knee arthroplasty (in Chinese). Chin J Joint Surg (Electron Ed) 2014;8:91-5. doi: 10.3877/cma.j.issn.1647-134X.2014.01.017.
16. Zhang YZ, Pei GX, Lu S, Li ZJ, Zhao JM, Wang YW, *et al*. Establishing lower-extremity mechanical axis by computer-aided design and its application in total knee arthroplasty (in Chinese). Chin J Orthop 2013;33:1196-203. doi: 10.3760/cma.j.issn.0253-2352.2013.12.005.
17. Zheng GY. Unifying energy minimization and mutual information maximization for robust 2D/3D registration of X-ray and CT images. Pattern Recognit 2007;4713:547-57. doi: 10.1007/978-3-540-74936-3_55.
18. Bingham J, Li G. An optimized image matching method for determining *in-vivo* TKA kinematics with a dual-orthogonal fluoroscopic imaging system. J Biomech Eng 2006;128:588-95. doi: 10.1115/1.2205865.
19. Tomazevic D, Likar B, Slivnik T, Pernus F. 3-D/2-D registration of CT and MR to X-ray images. IEEE Trans Med Imaging 2003;22:1407-16. doi: 10.1109/TMI.2003.819277.
20. Yamazaki T, Watanabe T, Nakajima Y, Sugamoto K, Tomita T, Yoshikawa H, *et al.* Improvement of depth position in 2-D/3-D registration of knee implants using single-plane fluoroscopy. IEEE Trans Med Imaging 2004;23:602-12. doi: 10.1109/TMI.2004.826051.
21. Chen Y, Gao D, Nie C, Luo L, Chen W, Yin X, *et al.* Bayesian statistical reconstruction for low-dose X-ray computed tomography using an adaptive-weighting nonlocal prior. Comput Med Imaging Graph 2009;33:495-500. doi: 10.1016/j.compmedimag.2008.12.007.
22. Chen Y, Ma JH, Feng QJ, Luo LM, Shi PC, Chen WH. Nonlocal prior Bayesian tomographic reconstruction. J Math Imaging Vis 2008;30:133-46. doi: 10.1007/s10851-007-0042-5.
23. Anderst W, Zauel R, Bishop J, Demps E, Tashman S. Validation of three-dimensional model-based tibio-femoral tracking during running. Med Eng Phys 2009;31:10-6. doi: 10.1016/j.medengphy.2008.03.003.
24. DeFrate LE, Sun H, Gill TJ, Rubash HE, Li G. *In vivo* tibiofemoral contact analysis using 3D MRI-based knee models. J Biomech 2004;37:1499-504. doi: 10.1016/j.jbiomech.2004.01.012.
25. Delp SL, Stulberg SD, Davies B, Picard F, Leitner F. Computer assisted knee replacement. Clin Orthop Relat Res 1998;354:49-56.
26. Komistek RD, Dennis DA, Mahfouz M. *In vivo* fluoroscopic analysis of the normal human knee. Clin Orthop Relat Res 2003;410:69-81. doi: 10.1097/01.blo.0000062384.79828.3b.
27. Li G, Wuerz TH, DeFrate LE. Feasibility of using orthogonal fluoroscopic images to measure *in vivo* joint kinematics. J Biomech Eng 2004;126:314-8. doi: 10.1115/1.1691448.
28. Van de Velde SK, Hosseini A, Kozánek M, Gill TJ, Rubash HE, Li G.

Application guidelines for dynamic knee joint analysis with a dual fluoroscopic imaging system. Acta Orthop Belg 2010;76:107-13.
29. Zhu Z, Li G. Construction of 3D human distal femoral surface models using a 3D statistical deformable model. J Biomech 2011;44:2362-8. doi: 10.1016/j.jbiomech.2011.07.006.
30. Wang S, Passias P, Li G, Li G, Wood K. Measurement of vertebral kinematics using noninvasive image matching method-validation and application. Spine (Phila Pa 1976) 2008;33:E355-61. doi: 10.1097/BRS.0b013e3181715295.
31. Baka N, Kaptein BL, de Bruijne M, van Walsum T, Giphart JE, Niessen WJ, *et al.* 2D-3D shape reconstruction of the distal femur from stereo X-ray imaging using statistical shape models. Med Image Anal 2011;15:840-50. doi: 10.1016/j.media.2011.04.001.
32. Zheng G, Gollmer S, Schumann S, Dong X, Feilkas T, González Ballester MA. A 2D/3D correspondence building method for reconstruction of a patient-specific 3D bone surface model using point distribution models and calibrated X-ray images. Med Image Anal 2009;13:883-99. doi: 10.1016/j.media.2008.12.003.